

# Radioactive Probes of the Supernova-Contaminated Solar Nebula: Evidence that the Sun was Born in a Cluster

Leslie W. Looney, John J. Tobin, and Brian D. Fields

*Department of Astronomy, University of Illinois at Urbana-Champaign, IL 61801*

## ABSTRACT

We construct a simple model for radioisotopic enrichment of the protosolar nebula by injection from a nearby supernova, based on the inverse square law for ejecta dispersion. This idealized model concisely and explicitly connects the observational data to the key astrophysical parameters; as such, it provides a useful tool for parameter studies that can inform the computationally expensive numerical (magneto)hydrodynamic studies essential for a full solution to this problem. We find that the presolar radioisotopes abundances (i.e., in solar masses) demand a nearby supernova: its distance  $D$  can be no larger than  $D/R_{\text{SS}} \leq 66$  times the size  $R_{\text{SS}}$  of the protosolar nebula, at a 90% confidence level, assuming  $1 M_{\odot}$  of protosolar material. The relevant size of the nebula depends on its state of evolution at the time of radioactivity injection. In one scenario, a collection of low-mass stars, including our sun, formed in a group or cluster with an intermediate- to high-mass star that ended its life as a supernova while our sun was still a protostar, a starless core, or perhaps a diffuse cloud. Using recent observations of protostars to estimate the size of the protosolar nebula constrains the distance of the supernova to  $D \sim 0.02$  pc to 1.6 pc. The supernova distance limit is consistent with the scales of low-mass stars formation around one or more massive stars, but it is closer than expected were the sun formed in an isolated, solitary state. Consequently, if *any* presolar radioactivities originated via supernova injection, we must conclude that our sun was a member of such a group or cluster that has since dispersed, and thus that solar system formation should be understood in this context. In addition, we show that the timescale from explosion to the creation of small bodies was on the order of 1.8 Myr (formal 90% confidence range of 0 to 2.2 Myr), and thus the temporal choreography from supernova ejecta to meteorites is important. Finally, we can not distinguish between progenitor masses from 15 to 25  $M_{\odot}$  in the nucleosynthesis models; however, the 20  $M_{\odot}$  model is somewhat preferred.

*Subject headings:* Sun: abundances; Sun: general; stars: formation; stars: circumstellar matter; stars: pre-main sequence; nuclear reactions, nucleosynthesis, abundances

## 1. Introduction

The picture of star formation that has been developed over the last few decades provides a good broad-brush explanation of isolated, low-mass, Sun-like star formation (e.g. Shu et al. 1993). However, is that picture valid for the formation of the Sun? The scenario is probably unlikely as there is good evidence that the majority of Sun-like stars form in clusters (e.g., Carpenter 2000; Lada & Lada 2003). In addition, the theoretical view that protostars form in relative isolation from their molecular cloud neighbors is also weakening (e.g., Clark et al. 2005).

To better explain the origin of the Sun and Planets, it is important to first understand the initial conditions in which the Sun formed. Did the Sun form in isolation or in a small group or cluster of stars that has since dispersed? The concept of a lonely Solar System birth has been challenged by the idea that the Sun was born near at least one massive star, in a group or cluster of stars, based on the study of short-lived radioisotopes in meteorites (e.g. Hester et al. 2004).

The main evidence for short-lived radioactive species is from isotopic anomalies of daughter species in primitive meteorites (for recent reviews, see Goswami & Vanhala 2000; Meyer & Clayton 2000; Wadhwa et al. 2006). The isotopes are now extinct, but they must have been live, and in relatively high abundances, during the early stages of planet formation in our Solar System. Possible origins for the measured isotopic abundances are that the Sun formed in a location that was enriched either by a stellar wind or a recent core-collapse supernova (e.g. Lee et al. 1977), hence in or near a cluster or stellar group environment. Other possibilities for the short-lived radioactive isotopes include irradiation in the circumstellar disk (e.g., Lee et al. 1998) or mixing of ejecta from core-collapse supernova in the interstellar medium (ISM) (e.g., Meyer & Clayton 2000; Hester & Desch 2005; Ouellette et al. 2005). However, new results reveal that the early Solar System contained significant amounts of the short-lived  $^{60}\text{Fe}$  radionuclide (e.g. Tachibana & Huss 2003; Mostefaoui et al. 2005) that can not be explained with the irradiation models or ISM mixing models (e.g. Tachibana & Huss 2003; Gounelle et al. 2006).

In this paper, we make the assumption that a supernova event occurred near the early solar nebula, such that short-lived radioactive species were injected into the solar nebula (e.g. Cameron & Truran 1977; Goswami & Vanhala 2000). Although, the  $^{60}\text{Fe}$  abundance could also be explained by ejecta from Asymptotic Giant Branch (AGB) stars, novae, or Type I supernovae, the likelihood of such late stellar stage objects overlapping with a star formation region is much smaller than a supernova that was born in the same cluster (e.g. Kastner & Myers 1994; Hester & Desch 2005).

With the assumption of a nearby supernova, we construct a simple model that directly and explicitly relates the observed pre-solar radioisotope abundances to the supernova distance and the size of the protosolar nebula into which they were injected. Our model, while idealized, clearly illustrates that the radioisotope abundances directly constrain (and in particular, place an upper limit on) the ratio of the supernova distance to the size of the nebula. This type of model has been discussed before (e.g. Vanhala & Boss 2000, 2002; Ouellette et al. 2005) with more emphasis on the detailed hydrodynamics of the injection of supernova material into the nebula. In this paper, we focus on a statistical parameter study, with emphasis on the supernova distance  $D$ . Our simple model allows for a rapid search of the parameter space and shows that in most scenarios, a nearby supernova (i.e.,  $D \leq$  a few pc, and  $\ll 1$  kpc) is required if *any* radioisotopes came from a supernova. This has important qualitative implications for the nature of the Sun’s formation, and quantitatively our results can inform and calibrate the more computationally expensive hydrodynamics calculations needed to solve the problem in all of its detail.

## 2. Supernova Radioisotope Injection into the Protosolar Nebula

The abundance of radioisotopes injected by a supernova explosion depends on—and thus probes—the properties of the Type II core-collapse supernova and its explosion, the propagation of the supernova remnant and entrained ejecta, and the ability of the protosolar nebula to capture the ejecta that impinge on it. Each of these aspects of the problem are known to be quite complex in its details (e.g. Chevalier 2000; Meyer & Clayton 2000; Vanhala & Boss 2000, 2002), and a full understanding of the problem must embrace this richness. Nonetheless, a simplified analytic treatment of the parameter space of the problem not only offers physical insight, but also provides a benchmark for comparison with the more elaborate descriptions.

### 2.1. Radioactivity Distance

In this spirit, we adopt the following idealized model (also see, Vanhala & Boss 2000; Ouellette et al. 2005). We assume a supernova event occurred at a distance  $D$  from the early solar nebula. The ejecta from the supernova blast is then spread with a “flux” (in fact, surface density) that follows the inverse square law. It then follows that the mass fraction  $X_i = M_{\text{SS},i}/M_{\text{SS}}$ , of a radionuclide  $i$ , observed in the Solar System is

$$X_i = f_{\text{inj}} \frac{M_{\text{SN},i}}{M_{\text{SS}}} \frac{\pi R_{\text{SS}}^2}{4\pi D^2} e^{-t/\tau_i} \quad (1)$$

where  $M_{\text{SS},i}$  is the mass of radionuclide  $i$  in the early solar system,  $M_{\text{SS}}$  is the effective “target” or “absorbing” mass of the solar nebula,  $M_{\text{SN},i}$  is the amount of radionuclide  $i$  produced in the supernova, and  $R_{\text{SS}}$  is the solar system radius. The exponential term accounts for the decay of the radionuclide, with decay constant  $\tau_i$ , in the time interval  $t$  between the supernova explosion and solar system formation (more precisely, until meteorite formation). Finally, the  $f_{\text{inj}} \leq 1$  measures the “injection efficiency,” i.e., the ratio of incident supernova radioisotope debris that is actually incorporated into the nebula. For example, Vanhala & Boss (2000) discuss the injection process in detail suggesting that in some cases the injection occurs via Rayleigh-Taylor instabilities with an efficiency of approximately  $f \simeq 0.1$ .

This model is simplified, and thus idealized, by assuming not only spherical, homogenous ejecta from isotropical supernova ejecta, but also that the supernova ejecta will be completely integrated and well mixed in the solar system material. On the other hand, the model readily provides insight into the proximity of the supernova that ejected the short-lived isotopes into the early solar nebula.

From Equation 1, we can derive a measure of “radioactivity distance”, which is the ratio of the supernova distance to the solar nebula radius.<sup>1</sup>

$$\frac{D}{R_{\text{SS}}} = \frac{1}{2} \sqrt{f_{\text{inj}} \frac{M_{\text{SN},i}}{X_i M_{\text{SS}}}} e^{-t/2\tau_i} = 100 f_{\text{inj}}^{1/2} e^{-t/2\tau_i} \left( \frac{M_{\text{SN},i}}{10^{-4} M_{\odot}} \right)^{1/2} \left( \frac{10^{-9}}{X_i} \right)^{1/2} \left( \frac{1 M_{\odot}}{M_{\text{SS}}} \right)^{1/2} \quad (2)$$

where the fiducial values are appropriate for  $^{60}\text{Fe}$  and  $1 M_{\odot}$  of solar nebula material. In other words, the radioactivity distance is only dependent on four variables. Arguably, the two with the largest uncertainties are the supernova yields  $M_{\text{SN},i}$  and presolar radioisotope abundance  $X_i$ . The supernova yields  $M_{\text{SN},i}$  are gathered from models of nucleosynthesis in massive stars (e.g., Woosley & Weaver 1995; Rauscher et al. 2002), which depend chiefly on the mass of the progenitor star. It is interesting to note that the input parameters appear under a square root in the expression for radioactivity distance, which is correspondingly less sensitive to errors in the inputs.

The abundance at isotopic closure of a once-live radionuclide parent  ${}^i\mathcal{P}$  is obtained from meteoritic measurement of anomalous abundances in its daughter product  ${}^i\mathcal{D}$ , where the decay scheme is  ${}^i\mathcal{P} \rightarrow {}^i\mathcal{D}$  (see recent review, Wadhwa et al. 2006). This procedure yields the initial ratio  ${}^i\mathcal{P}/\mathcal{P}_{\text{ref}}$  of the radioactive parent nuclide to a stable (and abundant) reference isotope  $\mathcal{P}_{\text{ref}}$  of the same atomic species. For example, studies of  $^{60}\text{Ni}$  excesses in meteorites

---

<sup>1</sup>The radioactivity distance is a close analog of a luminosity distance: radioisotope nucleosynthetic yield  $M_{\text{SN},i}$  takes the role of luminosity, and solar abundance (in fact, surface density  $M_{\text{SS},i}/\pi R_{\text{SS}}^2$ ) takes the role of observed flux.

give a measure of the pre-solar  $^{60}\text{Fe}/^{56}\text{Fe}$  ratio (e.g. Tachibana & Huss 2003; Mostefaoui et al. 2005; Tachibana et al. 2006).

Table 1 lists the short-lived radionuclides in the early solar nebula that are most likely to be contaminated by a Type II supernova ejecta (e.g. Wadhwa et al. 2006). We have excluded  $^{92}\text{Nb}$  and  $^{244}\text{Pu}$  since the former has very large uncertainties and the latter is not predicted in the two models used in our analysis. The ratios used are for the initial solar system abundance, which is defined at the creation of the calcium-aluminum-rich inclusions (CAIs), not necessarily at isotopic closure. This, however, creates difficulties when referencing the age at isotopic closure to the initial solar system abundance for some radionuclides. The  $^{36}\text{Cl}/^{35}\text{Cl}$  and  $^{41}\text{Ca}/^{40}\text{Ca}$  ratios are impacted the most from this uncertainty and may be considered lower limits (e.g., Wadhwa et al. 2006).

To recover the observed mass fraction for the presolar nebula (Table 1), we use the expression

$$X_i = \frac{{}^i\mathcal{P}}{\mathcal{P}_{\text{ref}}} \frac{\mathcal{P}_{\text{ref}}}{\text{H}} A_i X_{\text{H}} \quad (3)$$

where  $A_i$  is the atomic weight of the isotope. The early solar  $\mathcal{P}_{\text{ref}}/\text{H}$  abundance and the hydrogen mass fraction  $X_{\text{H}} = 0.711$  were taken from Lodders (2003), Table 2, where the associated uncertainties from the meteoritic ratios and abundances have been propagated. In most cases, the largest uncertainty is from the meteoritic ratios; the exception of which is the radionuclide ratio  $^{129}\text{I}/^{127}\text{I}$ , which has a large abundance uncertainty.

For the supernova radioisotope yields  $M_{\text{SN},i}$ , we use the results of theoretical models. To illustrate the (significant) uncertainties in these difficult calculations, we will compute results using both the model of Woosley & Weaver (1995) (at solar metallicity), which spans the mass progenitor range  $11 - 40M_{\odot}$ , and that of Rauscher et al. (2002), which updates much of the physics of the earlier model, but spans a narrower mass range. The model uncertainties are clearly large: for a given progenitor mass, the yields for the same isotope in the two models can diverge in some cases by as much as a factor of ten. We thus believe it is not overly conservative to adopt an uncertainty on the model yields as  $\sigma_{M_{\text{SN},i}} = M_{\text{SN},i}$ , i.e., a factor of two.

In addition, although a supernova can probably occur with stellar masses of 8 to  $10M_{\odot}$ , and indeed the lower mass supernova may be the most likely for the case of the Sun, the fate of these stars, and their nucleosynthesis, remains unclear. The main reason is that the lower mass objects are likely to behave differently than the standard core collapse SNe with more associated  $r$ -processed material (Wheeler et al. 1998). Unfortunately, these systems are not well studied, so not further discussed in this paper. Only the mass range of  $11 - 25M_{\odot}$  is considered, which provides results for low-mass supernovae and an overlap

of the two nucleosynthesis models. The 30, 35, and 40  $M_{\odot}$  models in Woosley & Weaver (1995) provide flat yields in comparison to the 25  $M_{\odot}$  model, with the exception of  $^{53}\text{Mn}$  that varies significantly depending on the assumed kinetic energy.

## 2.2. Results

In this section, we present numerical results for the radioactivity distance ratio  $D/R_{\text{SS}}$ . We will assume a perfect injection efficiency  $f_{\text{inj}} = 1$  and a solar system nebula mass  $M_{\text{SS}} = 1M_{\odot}$ , in both the text and figures, and we will revisit these assumptions in our discussion. Note that the results can be scaled for other efficiencies or masses via  $D/R_{\text{SS}} \propto f_{\text{inj}}^{1/2}$  or  $D/R_{\text{SS}} \propto M_{\text{SS}}^{-1/2}$ . In §3, these results will be applied to two basic cases: (1) injection into a core or circumstellar envelope, where  $f_{\text{inj}} \simeq 0.1$ ,  $M_{\text{SS}} \simeq 1M_{\odot}$ , and  $R_{\text{SS}} \simeq 0.05$  pc; and (2) injection into a circumstellar disk, where  $f_{\text{inj}} \simeq 1$ ,  $M_{\text{SS}} = M_{\text{disk}} \simeq 0.01M_{\odot}$ , and  $R_{\text{SS}} \simeq 100$  AU.

Figure 1 shows the radioactivity distance for the nine short-lived radioactive isotopes tabulated in Table 1, for the case  $t/\tau_i \ll 1$  of negligible delay between radioisotope nucleosynthesis and incorporation into meteorites. Both nucleosynthesis models are shown: the Rauscher et al. (2002) model with solid lines and the Woosley & Weaver (1995) model with dashed lines. As the figure is already complicated, the error bars on the Woosley & Weaver (1995) model are not drawn. Broadly speaking, the order of magnitude of the results are in line with the fiducial estimate in Equation (2), spanning  $D/R_{\text{SS}} \sim 10^1 - 10^3$ . We immediately see that if *any* pre-solar radioisotopes originated in a supernova, then (1) the explosion had to be close, within 10-10000 solar nebula radii; and (2) the supernova had to be recent,  $t/\tau_i \lesssim 1$ , else many of the shortest lived radioisotopes would have decayed and/or the required distance would become unfeasibly close.

In more detail, the large range of radioactivity distance in Figure 1 illustrates the complexity of the problem and the uncertainties in such a model. The nucleosynthesis uncertainties alone are clearly very large, as the two supernova models lead to distance estimates that can vary by factors as high as  $\sim 3$ . In the ideal case, in which all radioisotopes did originate in a supernova as described in the model, one would expect the curves for all isotopes to converge to a single unique value at some progenitor mass; this is not the case. In fact, it is clear from Figure 1 that the mass of the progenitor is unconstrained. Nonetheless, the majority of the isotopes are clustered near the middle of the graph, with some isotopes preferring larger radioactive distances ( $^{41}\text{Ca}$  and  $^{53}\text{Mn}$ ) and smaller radioactive distances ( $^{146}\text{Sm}$ ).

Two possible explanations for the stratification in Figure 1 suggest themselves: multiple sources of short-lived radioisotopes and decay of the radioisotopes. We have thus far considered the case of a supernova as the unique source of presolar radioactivities, but other sources certainly are possible and indeed must be present at some level. One source is the abundance of radioisotopes in the general interstellar medium, which achieves a steady state between production and decay. The steady-state abundance is essentially the production abundance, reduced by the ratio  $\tau_i/\tau_\star$  of decay time to a star-formation time  $\tau_\star$  appropriate for the global ISM. Consequently, the highest steady-state abundances will be those of long-lived species, such as  $^{53}\text{Mn}$ ,  $^{146}\text{Sm}$ ,  $^{107}\text{Pd}$ , and  $^{129}\text{I}$  and others (Meyer & Clayton 2000).

Another more promising source of presolar radioisotopes is *in situ* production through protostellar cosmic rays in the circumstellar disk ( $^{41}\text{Ca}$  and  $^{53}\text{Mn}$ ; Lee et al. 1998). Indeed, the presence of presolar  $^{10}\text{Be}$  (McKeegan et al. 2000) suggests that this may well be the case, since this isotope is in general only produced by cosmic rays, and not at all by supernovae (e.g., Vangioni-Flam et al. 1996). We note that there should also be a steady-state  $^{10}\text{Be}$  abundance in the general ISM. If cosmic-ray bombardment occurs over a timescale  $\tau_\star \gg \tau_{10} = 2.2$  Myr, then immediately afterwards, the  $^{10}\text{Be}$  abundance relative to the stable isotope is  $^{10}\text{Be}/^9\text{Be} \sim \tau_{10}/\tau_\star \sim 10^{-3}(1 \text{ Gyr}/\tau_\star)$ . To explain the full pre-solar value  $^{10}\text{Be}/^9\text{Be} \sim 10^{-3}$  (McKeegan et al. 2000) would seem to require an effective Galactic cosmic-ray nucleosynthesis timescale of  $\tau_\star \sim 1$  Gyr, which is short compared to the  $\sim 9$  Gyr cosmic age at the solar birth. In addition to this Galaxy-wide beryllium production, the nascent Solar System was likely subject to transient and localized enhancements in Galactic (i.e., high-energy) cosmic rays that would lead to some level of enhancement in spallation radioisotope production (Fields et al. 1996). We note that a nearby supernova represents a local cosmic-ray accelerator. In addition, as the protosolar core collapses, it becomes opaque to the already high flux of  $^{10}\text{Be}$  Galactic cosmic-rays and traps them (Desch et al. 2004). Nonetheless,  $^{60}\text{Fe}$  is still the one isotope not produced at the needed levels in the cosmic-ray scenario, and thus points to the need for at least *some* supernova material (e.g., Hester & Desch 2005).

In any case, local production (and/or other extra sources, including the possibility of multiple supernovae) would mean that the presolar radioisotope abundance  $X_i$  would have two, or more, components. In those conditions, the radioactivity distances estimated in this paper will, by definition, be lower limits to the supernova distance. To disentangle these sources is not a trivial task, but not hopeless either, as we are aided by (1) the wide range of radioisotope lifetimes, and (2) the rather different abundance patterns arising from the various nucleosynthesis mechanisms. For example, if there is a significant local cosmic-ray production of, say,  $^{26}\text{Al}$ , this would reveal itself as an anomalously low radioactivity distance for this isotope relative to a supernova-only species such as  $^{60}\text{Fe}$ . Such an analysis is beyond the scope of this paper.

Based on probable secondary sources, we exclude  $^{146}\text{Sm}$  from the parameter study in §2.3. The isotope has the longest half-life in Table 1 by almost a factor of three. As suggested by Meyer & Clayton (2000), meteoritic measurements of  $^{146}\text{Sm}$  are most likely contaminated by a steady-state component in the ISM maintained by Type Ia supernovae. If the abundance is increased, the derived radioactive distance decreases in Equation 2, which explains its location at the bottom of Figure 1. On the other hand,  $^{53}\text{Mn}$ , although within the error bars of  $^{60}\text{Fe}$ , demands a high radioactive distance. Yet, like  $^{146}\text{Sm}$ , the measured  $^{53}\text{Mn}$  abundance is expected to have been contaminated by the steady-state ISM abundance (Meyer & Clayton 2000), implying an even larger distance for the supernova. However,  $^{53}\text{Mn}$  is produced during explosive silicon burning, which occurs at the very end of the supernova process. Because the Type-II supernova explosion mechanism is still poorly understood, it is difficult to accurately predict the products of explosive silicon burning (Woosley et al. 2002). In addition, the overabundance of  $^{53}\text{Mn}$  in the supernova ejecta has been explained by the probable fallback of the innermost layers of the star (Meyer 2005). For these reasons, we also exclude  $^{53}\text{Mn}$  from the parameter study in §2.3.

Finally, within the context of the model in this paper, the radioactivity distance estimates for each species will vary due to the effect of radioactive decay, if there is any significant time delay between nucleosynthesis and incorporation into meteorites. Of course, for any material injected by a nearby supernova, *some* time must inevitably elapse between radioisotope production and incorporation into meteorites, in particular the CAIs. At minimum, there must be a nonzero time-of-flight between the supernova and the presolar nebula; also, the time for creation of small bodies should be  $\sim 1$  to 10 Myrs based on circumstellar disk lifetimes (e.g., Hartmann 2005). If the supernova impact itself initiated the collapse or merely seeded a nearby cloud of the presolar nebula (Cameron & Truran 1977), then there is an additional delay due to the collapse, which is estimated to take  $\sim 0.1$  to 10 Myrs (e.g., Shu et al. 1993; Vanhala & Cameron 1998; Vanhala & Boss 2000; Tassis & Mouschovias 2004).

Any delay would imply that the supernova radioisotope signal is underestimated, and correcting for this effect decreases the radioactivity distance in Equation (2). Thus, the un-delayed results of Figure 1 represent *upper limits* to the distance. However, adjustment to the radioactive distance is exponentially sensitive to the isotope lifetime; the shorter-lived species such as  $^{41}\text{Ca}$  and  $^{36}\text{Cl}$  will vary strongly for modest delays of  $\sim 100$  kyr, while the longer-lived species ( $\tau \gtrsim 5$  Myr) will be essentially unaffected over timescales appropriate for the full ensemble of isotopes. For example, this explains why  $^{41}\text{Ca}$  demands the largest radioactivity distance in Figure 1;  $^{41}\text{Ca}$  has decayed the most. On the other hand, because of their short half-lives the initial  $^{41}\text{Ca}$  and  $^{36}\text{Cl}$  abundances are also among the most difficult to determine (e.g., Wadhwa et al. 2006). Indeed, their estimated abundances in Table 1 are



really lower limits, which implies upper limits in Figure 1.

### 2.3. Parameter Modeling

In order to comment on the degree of concordance in Figure 1, we define the  $\chi^2$  of the data at each progenitor mass with assumed radioactivity distance  $(D/R_{SS})_{\text{guess}}$  to be

$$\chi^2(M_{\text{SN}}) = \sum_i \frac{[(D/R_{SS})_i - (D/R_{SS})_{\text{guess}}]^2}{\sigma_i^2} . \quad (4)$$

We evaluated a grid of  $\chi^2$  values for  $(D/R_{SS})_{\text{guess}}$  ranging from 1 to 200, in steps of 1. For each nucleosynthesis model and progenitor mass, a separate  $\chi^2$  value was calculated. In addition, a decay time ranging from 0 to 2.5 Myrs, in steps of 0.1 Myrs, was included. This gives a total of 5200 possible combinations for each progenitor mass. A parameter set was considered an acceptable fit at a 90% confidence level, i.e. likelihoods  $> 10\%$ .

Due to the large uncertainty in the data and nucleosynthesis models, there is a large range of acceptable fits. The Rauscher et al. (2002) supernova nucleosynthesis model, with the larger number of predicted isotopes but smaller mass range, has the largest constraints on the parameters. Therefore, we will discuss those fits in detail. Figure 2 shows the calculated likelihoods of the parameter study. The lowest contours in Figure 2 are 10%.

With accepted likelihoods greater than 10%, the mass is not well constrained (i.e. all mass models fit); however, it is clear that the mass model of 20  $M_{\odot}$  is the highly preferred model. In fact, the best fit (likelihood of 93%) is with a progenitor mass of 20  $M_{\odot}$ , decay time of 1.8 Myrs, and a  $D/R_{SS}$  ratio of 22. However, it is important to keep in mind that all fits in Figure 2 are statistically equivalent in our 90% confidence level. Although the preferred  $\chi^2$  of the 20  $M_{\odot}$  model is perhaps intriguing and should be explored more in detail, it is probably a conspiracy of terms. The tangible reason that the 20  $M_{\odot}$  model fits the data so well is due to the increased predicted abundance of  $^{41}\text{Ca}$  and  $^{36}\text{Cl}$  in that model. It is crucial to remember that the strict meteoritic data for  $^{41}\text{Ca}$  and  $^{36}\text{Cl}$  are upper limits, which can heavily impact the result by decreasing the decay time necessary to achieve an overlap. Figure 3 shows the radioactive distance at four different decay times,  $t = 0, 0.1, 1.8,$  and 2 Myrs,  $t = 1.8$  Myrs was included as it is the best fit time. The figure illustrates the evolution with different decay times.

It is clear from the above discussion that the most constrained aspect of the simplified problem is the radioactivity distance with some constraint on the decay time. Using a 90%

confidence level, the distance ratio and decay time is constrained to be

$$5 < D/R_{SS} < 66 \tag{5}$$

and

$$0 < \tau < 2.2 \text{ Myrs}, \tag{6}$$

respectively, using the Rauscher et al. (2002) nucleosynthesis model. In order to compare the distance ratio to other distance estimates, we have to use assumptions for the early solar system mass and radius. The large time range is unsurprisingly consistent with many other estimated time scales (e.g., Meyer et al. 2003; Meyer 2005; Ouellette et al. 2005).

### 3. Implications for the Presolar Environment

The largest assumption in Figure 3 is that a supernova exploded nearby the protosolar nebula such that up to 2.2 Myrs later those isotopes were incorporated into meteorites. The simplest and most probable explanation is that our Sun formed in a loose cluster containing a massive star that later dispersed. In that case, was the Sun triggered by the supernova (e.g., Cameron & Truran 1977), or did it form at a similar time as the progenitor star (e.g., Chevalier 2000)?

One must keep in mind that the temporal choreography is crucial to this discussion. Our results show that the time scale for the isotopic inclusion into solid objects ranges from 0 to 2.2 Myrs, including travel, grain growth, and planetesimal formation. That is a particularly quick timescale when compared to the lifetime of a protostar. In addition, if we consider that the expected timescale for large body formation occurs at the end of the protostellar lifetime, during the Class II/III stage or later (e.g., Hartmann 2005), then the likelihood of this particular supernova triggering our solar system does exist, but it must evolve quickly. Nonetheless, we discuss these scenarios using the current best estimates of early nebula radius and mass.

#### 3.1. Siblings at Birth

In the case of siblings, the protosun and the progenitor star are formed on similar time scales (within  $\sim 1$  Myrs, Lada & Lada 2003): possibly a birth case similar to the cluster of about 1600 low-mass young stars in the Orion Nebula within  $\sim 2$  pc of the the Trapezium group (core radius of 0.2 pc, Hillenbrand & Hartmann 1998). Within the inner 0.4 pc, 85% of the stars have L-band excesses that suggest circumstellar disks (Lada et al. 2000). In

spite of the harsh environment near the massive cluster, the low-mass young stars near the central star  $\theta^1$  Ori C have observable disks due to the photoionization effects of the massive star (e.g., McCaughrean & O’dell 1996).

Clearly from Figures 2 and 3, the isotopic evidence does not well constrain the mass of the progenitor star. Nonetheless, the main sequence lifetime of the progenitor star can be estimated from recent models (e.g., Romano et al. 2005) as 7 to 10 Myrs for the mass range in Figure 3. In addition to the main sequence lifetime, one must include the protostellar lifetime of the massive star. Although this value is poorly known, the best estimates range from  $10^4$  to  $10^5$  years (e.g., Yorke 1986; McKee & Tan 2002), a fraction of the main sequence lifetime.

Although the time frame of  $\sim 10$  Myrs is significant, low-mass stars evolve at a much slower pace than higher mass stars. In fact, the longest stage may be before collapse even begins on the order of the ambipolar diffusion timescale, which ranges from 0.1 to 10 Myrs, depending on the initial mass-to-flux ratio and degree of ionization in the cloud (e.g., Tassis & Mouschovias 2004). That in combination with the standard spread of ages in clusters of  $\sim 1$  Myrs (Lada & Lada 2003) implies that the protostellar nebula could have been in many possible evolutionary stages (also see Hester & Desch 2005): (1) the youngest protostellar evolution stage, the so-called Class 0 stage, which is dominated by an circumstellar envelope that implies  $R_{SS} \simeq 5000$  AU and  $M_{SS} \simeq 1 M_{\odot}$  (e.g., Looney et al. 2000, 2003). Although the injection efficiency is probably closer to 10% (Vanhala & Boss 2002), we conservatively use  $f_{inj} \simeq 1$  (i.e., larger distance); or (2) an older protostar, Class I/II, dominated by the circumstellar disk that implies  $R_{SS} \simeq 100$  AU and  $M_{SS} \simeq 0.02 M_{\odot}$  (e.g., Looney et al. 2000), which is similar to the minimum mass solar circumstellar disk (e.g., Weidenschilling 1977). We conservatively assume a large injection efficiency of  $f_{inj} \simeq 1$ .

From our analysis in §2.3, the radioactivity distance ranges from 5 to 66. Using that range of radioactivity distance ratio fits with the above size and mass estimates, yields distances of 0.12 to 1.6 pc and 0.02 to 0.22 pc, respectively (cf. Chevalier 2000; Ouellette et al. 2005). Note that a very low disk mass in older Class III sources or even debris disks would result in a supernova distance that is many pc away in this formalism (i.e.  $M_{SS}$  is very small). However, it is unclear how those systems could manufacture the meteorites necessary for the short lived isotope detection. The ejecta must be incorporated into the objects at an early enough time to be detected in meteorites. It is also important to note that these derived distances are very consistent with low-mass systems seen in clusters with large mass members (e.g., Orion or Eagle Nebula).

### 3.2. Triggered Birth

If we assume that a supernova event injected short lived isotopes into the early solar nebula, one must also consider that this event could have triggered the collapse of the nebula (e.g., Cameron & Truran 1977). Many recent models have shown that moderately slow shock waves (20-45 km/s) can trigger the collapse of cores (e.g., Boss 1995; Vanhala & Cameron 1998): too little and no collapse, too much and the core is torn apart. A quick collapse process ( $\sim 10^4 - 10^5$  yrs, Vanhala & Cameron 1998) may also account for the low radioactive distance (i.e. large  $X_i$ ) of the majority of the longer half-life isotopes ( $^{146}\text{Sm}$ ,  $^{129}\text{I}$ ,  $^{182}\text{Hf}$ , and  $^{107}\text{Pd}$ ) seen in Figure 1; the molecular cloud core in which the Sun formed would not have time to decay the initial ISM component. On the other hand, Hester & Desch (2005) argue that a supernova triggering a collapse and injecting that collapse with its radioisotopes, is probably less common than the scenario where supernova ejecta intercept a protostar.

In the triggering scenario, the solar nebula would not yet have evolved to a Class 0 protostar, implying two possible states: (1) a starless core, which has  $R_{\text{SS}} \simeq 7000$  AU and typical mass of  $M_{\text{SS}} \simeq 2 M_{\odot}$  (e.g., Kirk et al. 2005). Again, although the injection efficiency is probably closer to 10% (Vanhala & Boss 2002), we conservatively use  $f_{\text{inj}} \simeq 1$  (i.e., larger distance); or (2) a quickly triggered (e.g.  $< 1$  Myrs), diffuse cloud as modeled by a Bonner-Ebert sphere, considered by Vanhala & Boss (2000, 2002), with  $R_{\text{SS}} \simeq 0.06$  pc, mass of  $M_{\text{SS}} \simeq 1M_{\odot}$ , and  $f_{\text{inj}} \simeq 0.1$ . With these two possibilities, the estimated ranges of distances are 0.12 to 1.6 pc and 0.06 to 1.2 pc (or 0.3 to 4 pc for the overly conservative case of  $f_{\text{inj}} \simeq 1$ ), respectively. This can be compared to the values of Vanhala & Boss (2000, 2002), 5.2 to 26 pc. Vanhala & Boss (2000, 2002) comment on the mismatch of distance and offer possible resolutions. On the other hand, the possibility of a supernova inducing a quick collapse of a very diffuse cloud, i.e.,  $R_{\text{SS}} > 0.1$  pc, will significantly increase the derived distance to the supernova.

### 3.3. Travel Time

With an assumed ejecta speed of 30 km/s and the maximum estimated distances from above (e.g., 1.6 pc or even most conservatively 4 pc), the travel time can be estimated at  $\sim 5 \times 10^4$  and  $1 \times 10^5$  yrs, respectively. Using our best fit decay time of 1.8 Myrs, this implies that the ejecta material mixed with the solar nebula material until meteorites were produced. Given nearly 1.8 Myrs of residency within the solar nebula, it is possible that the SN ejecta would become homogenized in the cloud. This would be consistent with the formation timescale of calcium-aluminum-rich inclusions (CAIs), on the order of a million years (e.g., Wadhwa & Russell 2000).

#### 4. Conclusions

We present a simple model relating the pre-solar abundances of short-lived radioisotopes to the properties of the injecting supernova event. While our model is idealized, it is also explicit and computationally simple, yielding a parameter study whose general aspects are intriguing. In general, we are driven to conclude that a very nearby supernova event must be invoked if *any* presolar radioactivities are due to injection from a single explosion. Specifically, to a formal confidence level of 90%, the distance from the Solar Nebula and the supernova was in the range of 0.1 to 1.6 pc, for siblings and up to approximately 4 pc (in the most conservative, and unlikely, case of perfect injection) for triggered birth, using the Rauscher et al. (2002) nucleosynthesis models for 15 to 25  $M_{\odot}$  progenitors. This sounds surprisingly close, but it is consistent with typical distances found for low-mass stars clustering around one or more massive stars. We posit that our Sun was a member of such a cluster that has since dispersed.

It is important to note that our distance estimates imply that the Sun was directly influenced by the massive star’s photoionization effects, much like proplyds in Orion. To understand the Sun’s formation, one must include the large role played by such a complicated environment. The minimum distance is also interesting, as it is similar to the distance at which the disk would probably be destroyed  $< 0.25$  pc (Chevalier 2000). Our estimated distance range includes the expected uncertainties of the nucleosynthesis models and the radioisotopic measurements. Although the physical parameters of the solar nebula also play a large role in these estimates, we use nearly all protostellar evolutionary states to compile our range.

In addition to the distance of the supernova, we constrain the time scale of the explosion to the creation of small bodies to a 90% confidence range of 0 to 2.2 Myrs. The majority of this time was probably spent in our solar system during the building of small objects from the circumstellar dust; in fact, it is consistent with the estimates for chondrule production. It is important to note that the temporal choreography from supernova ejecta to meteorites is crucial. The upper limits of our fit decay times make it possible for the supernova to have triggered the fast collapse of our Sun, seeded it with short-lived isotopes, and created CAIs, but it seems more likely that the Sun was already a protostar during the explosion (e.g., Hester & Desch 2005).

In addition to the inherent uncertainties in our model, there are additional assumptions that would imply a smaller or larger supernova distance. There are two clear cases that would cause our deduced distances to be an upper limit: (1) an inclined circumstellar disk (Class I/II source) would have a lower cross-sectional area and not collect the full supernova contaminates as a face-on disk, and (2) the ejecta may not be effectively stopped by the

circumstellar disk as assumed ( $f_{\text{inj}} \ll 1$ ) (i.e., effectiveness of the injection process; see Vanhala & Boss 2002). Similarly, there are two opposing cases that would make our deduced distances lower limits: (1) highly inhomogeneous ejecta (i.e. bullets as seen in Cas A, Willingale et al. 2003) would not allow a predictable distance, and (2) although the material is injected uniformly onto the circumstellar disk, the inner regions of the disk has a higher density than the outer regions (e.g., Mundy et al. 1996), so if there is no mixing, the measured meteorites are produced *in situ* with abundances lower than expected. These crucial issues lie within the domain of sophisticated (magneto)hydrodynamical simulations that will yield a fuller understanding of this problem; our simple model serves as a tool that highlights and quantifies the issues that the full numerical models address.

In closing, we note that the analysis presented here for extinct presolar meteoritic radioactivities closely parallels considerations of live geological radioactivities as signatures of relatively recent nearby supernovae (e.g., Ellis et al. 1996; Knie et al. 2004). Both analyses leverage the uniqueness of radioisotopes as a signature of supernova activity, and both use the inverse square law in the same way to gauge distance. Moreover, Fields et al. (2005) emphasize that given a confirmed nearby supernova event, one can then turn the problem around, reading the presence or absence of, and detailed abundances of, all radioisotopes as direct probes of supernova ejecta and thus nucleosynthesis. This adds another way that meteoritic anomalies serve as fossil testimony to our massive sibling.

We thank You-Hua Chu, Charles Gammie, and Konstantinos Tassis for discussions. In particular, we thank the referee for significantly impacting the quality and usefulness of this paper. L.W.L. acknowledges support from the Laboratory for Astronomical Imaging at the University of Illinois, the National Science Foundation under Grant No. AST-0228953, and NASA under Origins grant No. NN06GE41G. B.D.F. acknowledges support by the National Science Foundation under Grant No. AST-0092939.

## REFERENCES

- Boss, A. P. 1995, ApJ, 439, 224
- Brazzle, R. H. 1999, Geochim. Cosmochim. Acta, 63, 739
- Cameron, A. G. W. & Truran, J. W. 1977, Icarus, 30, 447
- Carlson, R. W. & Hauri, E. H. 2001, Geochim. Cosmochim. Acta, 65, 1839
- Carpenter, J. M. 2000, AJ, 120, 3139

- Chevalier, R. A. 2000, *ApJ*, 538, L151
- Clark, P. C., Bonnell, I. A., Zinnecker, H., & Bate, M. R. 2005, *MNRAS*, 359, 809
- Cosarinsky, M., Taylor, D. J., & McKeegan, K. D. 2006, in 37th Annual Lunar and Planetary Science Conference, ed. S. Mackwell & E. Stansbery, 2357–+
- Desch, S. J., Connolly, Jr., H. C., & Srinivasan, G. 2004, *ApJ*, 602, 528
- Ellis, J., Fields, B. D., & Schramm, D. N. 1996, *ApJ*, 470, 1227
- Fields, B. D., Casse, M., Vangioni-Flam, E., & Nomoto, K. 1996, *ApJ*, 462, 276
- Fields, B. D., Hochmuth, K. A., & Ellis, J. 2005, *ApJ*, 621, 902
- Goswami, J. N. & Vanhala, H. A. T. 2000, *Protostars and Planets IV*, 963
- Gounelle, M., Shu, F. H., Shang, H., Glassgold, A. E., Rehm, K. E., & Lee, T. 2006, *ApJ*, 640, 1163
- Hartmann, L. 2005, in *ASP Conf. Ser. 341: Chondrites and the Protoplanetary Disk*, 131–+
- Hauri, E. H., Carlson, R. W., & Bauer, J. 2000, in *Lunar and Planetary Institute Conference Abstracts*, 1812–+
- Hester, J. J. & Desch, S. J. 2005, in *ASP Conf. Ser. 341: Chondrites and the Protoplanetary Disk*, ed. A. N. Krot, E. R. D. Scott, & B. Reipurth, 107–+
- Hester, J. J., Desch, S. J., Healy, K. R., & Leshin, L. A. 2004, *Science*, 304, 1116
- Hillenbrand, L. A. & Hartmann, L. W. 1998, *ApJ*, 492, 540
- Kastner, J. H. & Myers, P. C. 1994, *ApJ*, 421, 605
- Kirk, J. M., Ward-Thompson, D., & André, P. 2005, *MNRAS*, 360, 1506
- Kleine, T., Halliday, A. N., Palme, H., Mezger, K., & Markowski, A. 2006, in 37th Annual Lunar and Planetary Science Conference, ed. S. Mackwell & E. Stansbery, 1884–+
- Kleine, T., Mezger, K., Palme, H., & Scherer, E. 2005, in 36th Annual Lunar and Planetary Science Conference, ed. S. Mackwell & E. Stansbery, 1431–+
- Knie, K., Korschinek, G., Faestermann, T., Dorfi, E. A., Rugel, G., & Wallner, A. 2004, *Physical Review Letters*, 93, 171103

- Lada, C. J. & Lada, E. A. 2003, *ARA&A*, 41, 57
- Lada, C. J., Muench, A. A., Haisch, K. E., Lada, E. A., Alves, J. F., Tollestrup, E. V., & Willner, S. P. 2000, *AJ*, 120, 3162
- Lee, T., Papanastassiou, D. A., & Wasserburg, G. J. 1977, *ApJ*, 211, L107
- Lee, T., Shu, F. H., Shang, H., Glassgold, A. E., & Rehm, K. E. 1998, *ApJ*, 506, 898
- Lin, Y., Guan, Y., Leshin, L. A., Ouyang, Z., & Wang, D. 2005, *PNAS*, 102, 1306
- Lodders, K. 2003, *ApJ*, 591, 1220
- Looney, L. W., Mundy, L. G., & Welch, W. J. 2000, *ApJ*, 529, 477
- . 2003, *ApJ*, 592, 255
- Lugmair, G. W. & Galer, S. J. G. 1992, *Geochim. Cosmochim. Acta*, 56, 1673
- McCaughrean, M. J. & O'dell, C. R. 1996, *AJ*, 111, 1977
- McKee, C. F. & Tan, J. C. 2002, *Nature*, 416, 59
- McKeegan, K. D., Chaussidon, M., & Robert, F. 2000, *Science*, 289, 1334
- Meyer, B. S. 2005, in *ASP Conf. Ser. 341: Chondrites and the Protoplanetary Disk*, ed. A. N. Krot, E. R. D. Scott, & B. Reipurth, 515–+
- Meyer, B. S. & Clayton, D. D. 2000, *Space Science Reviews*, 92, 133
- Meyer, B. S., Clayton, D. D., The, L.-S., & El Eid, M. F. 2003, in *Lunar and Planetary Institute Conference Abstracts*, ed. S. Mackwell & E. Stansbery, 2074–+
- Mostefaoui, S., Lugmair, G. W., & Hoppe, P. 2005, *ApJ*, 625, 271
- Mundy, L. G., Looney, L. W., Erickson, W., Grossman, A., Welch, W. J., Forster, J. R., Wright, M. C. H., Plambeck, R. L., Lugten, J., & Thornton, D. D. 1996, *ApJ*, 464, L169+
- Nyquist, L. E., Shih, C.-Y., Wiesmann, H., Reese, Y., Ulyanov, A. A., & Takeda, H. 1999, in *Lunar and Planetary Institute Conference Abstracts*, 1604–+
- Ouellette, N., Desch, S. J., Hester, J. J., & Leshin, L. A. 2005, in *ASP Conf. Ser. 341: Chondrites and the Protoplanetary Disk*, ed. A. N. Krot, E. R. D. Scott, & B. Reipurth, 527–+



- Rauscher, T., Heger, A., Hoffman, R. D., & Woosley, S. E. 2002, *ApJ*, 576, 323
- Romano, D., Chiappini, C., Matteucci, F., & Tosi, M. 2005, *A&A*, 430, 491
- Shu, F., Najita, J., Galli, D., Ostriker, E., & Lizano, S. 1993, in *Protostars and Planets III*, 3–42937
- Srinivasan, G., Sahijpal, S., Ulyanov, A. A., & Goswami, J. N. 1996, *Geochim. Cosmochim. Acta*, 60, 1823
- Tachibana, S. & Huss, G. R. 2003, *ApJ*, 588, L41
- Tachibana, S., Huss, G. R., Kita, N. T., Shimoda, G., & Morishita, Y. 2006, *ApJ*, 639, L87
- Tassis, K. & Mouschovias, T. C. 2004, *ApJ*, 616, 283
- Vangioni-Flam, E., Casse, M., Fields, B. D., & Olive, K. A. 1996, *ApJ*, 468, 199
- Vanhala, H. A. T. & Boss, A. P. 2000, *ApJ*, 538, 911
- . 2002, *ApJ*, 575, 1144
- Vanhala, H. A. T. & Cameron, A. G. W. 1998, *ApJ*, 508, 291
- Wadhwa, M., Amelin, Y., Davis, A. M., Lugmair, G. W., Meyer, B., Gounelle, M., & Desch, S. 2006, *Protostars and Planets V*
- Wadhwa, M. & Russell, S. S. 2000, *Protostars and Planets IV*, 995
- Weidenschilling, S. J. 1977, *Ap&SS*, 51, 153
- Wheeler, J. C., Cowan, J. J., & Hillebrandt, W. 1998, *ApJ*, 493, L101+
- Willingale, R., Bleeker, J. A. M., van der Heyden, K. J., & Kaastra, J. S. 2003, *A&A*, 398, 1021
- Woosley, S. E., Heger, A., & Weaver, T. A. 2002, *Reviews of Modern Physics*, 74, 1015
- Woosley, S. E. & Weaver, T. A. 1995, *ApJS*, 101, 181
- Yorke, H. W. 1986, *ARA&A*, 24, 49
- Young, E. D., Simon, J. I., Galy, A., Russell, S. S., Tonui, E., & Lovera, O. 2005a, *Science*, 308, 223

Young, E. D., Simon, J. I., Galy, A., Russell, S. S., Tonui, E. K., & Lovera, O. 2005b, in 36th Annual Lunar and Planetary Science Conference, ed. S. Mackwell & E. Stansbery, 1525–+

Table 1. Adopted Short-lived Radioactive Isotopes

Radio- <sup>a</sup> isotope ${}^i\mathcal{P}$	Ref. $\mathcal{P}_{\text{ref}}$	$t_{1/2}$ (Myr)	Meteoritic <sup>b</sup> Ratio ${}^i\mathcal{P}/\mathcal{P}_{\text{ref}}$	Meteoritic <sup>b</sup> Uncert. $\sigma_{i\mathcal{P}}$	Reference <sup>c</sup> Abundance $\mathcal{P}_{\text{ref}}/\text{H}$	Reference <sup>c</sup> Uncert. $\sigma_{\mathcal{P}_{\text{ref}}}$	Mass Fraction $X_i$	Mass Uncert. $\sigma_{X_i}$
${}^{26}\text{Al}$	${}^{27}\text{Al}$	0.72	$5.9 \times 10^{-5}$	$0.6 \times 10^{-5}$	$3.46 \times 10^{-6}$	$0.16 \times 10^{-6}$	$3.77 \times 10^{-9}$	$0.42 \times 10^{-9}$
${}^{36}\text{Cl}$	${}^{35}\text{Cl}$	0.30	$1.6 \times 10^{-4}$	$0.7 \times 10^{-4}$	$2.15 \times 10^{-7}$	$0.29 \times 10^{-7}$	$8.82 \times 10^{-10}$	$4.04 \times 10^{-10}$
${}^{41}\text{Ca}$	${}^{40}\text{Ca}$	0.10	$1.4 \times 10^{-8}$	$0.1 \times 10^{-8}$	$2.59 \times 10^{-6}$	$0.18 \times 10^{-6}$	$1.06 \times 10^{-12}$	$0.10 \times 10^{-12}$
${}^{53}\text{Mn}$	${}^{55}\text{Mn}$	3.7	$2.8 \times 10^{-5}$	$0.3 \times 10^{-5}$	$3.77 \times 10^{-7}$	$0.26 \times 10^{-7}$	$3.98 \times 10^{-10}$	$0.51 \times 10^{-10}$
${}^{60}\text{Fe}$	${}^{56}\text{Fe}$	1.5	$7.5 \times 10^{-7}$	$2.5 \times 10^{-7}$	$3.45 \times 10^{-5}$	$0.24 \times 10^{-5}$	$1.10 \times 10^{-9}$	$0.38 \times 10^{-9}$
${}^{107}\text{Pd}$	${}^{108}\text{Pd}$	6.5	$2.0 \times 10^{-5}$	$0.2 \times 10^{-5}$	$5.90 \times 10^{-11}$	$0.41 \times 10^{-11}$	$8.98 \times 10^{-14}$	$1.09 \times 10^{-14}$
${}^{129}\text{I}$	${}^{127}\text{I}$	15.7	$1.1 \times 10^{-4}$	$0.1 \times 10^{-4}$	$4.10 \times 10^{-11}$	$1.13 \times 10^{-11}$	$4.14 \times 10^{-13}$	$1.20 \times 10^{-13}$
${}^{146}\text{Sm}$	${}^{144}\text{Sm}$	103	$7 \times 10^{-3}$	$2 \times 10^{-3}$	$1.05 \times 10^{-11}$	$0.10 \times 10^{-11}$	$7.60 \times 10^{-12}$	$2.28 \times 10^{-12}$
${}^{182}\text{Hf}$	${}^{180}\text{Hf}$	8.9	$1.1 \times 10^{-4}$	$0.1 \times 10^{-4}$	$6.99 \times 10^{-12}$	$0.64 \times 10^{-12}$	$9.95 \times 10^{-14}$	$1.28 \times 10^{-14}$

<sup>a</sup>Only those isotopes suspected to come from core-collapse supernovae (e.g., Wadhwa et al. 2006) are included, except  ${}^{92}\text{Nb}$  and  ${}^{244}\text{Pu}$ .  ${}^{92}\text{Nb}$  and  ${}^{244}\text{Pu}$  were omitted because of a very high uncertainty and a lack of predictions in the two supernovae ejecta models used in this paper, respectively. The ratio given here is the initial solar system abundance, which is measured at the creation of the CAIs, not necessarily at isotopic closure.

<sup>b</sup>Other references used are  ${}^{26}\text{Al}$ : Young et al. (2005a,b); Cosarinsky et al. (2006);  ${}^{36}\text{Cl}$ : Lin et al. (2005) (The ratio used is dependent on the  ${}^{26}\text{Al}/{}^{27}\text{Al}$  ratio in the measured mantle compared to the CAI. The ratio used was consistent, within the error bars, with our assumed value. However, the  ${}^{26}\text{Al}/{}^{27}\text{Al}$  ratio in the mantle was not well detected, so this value is more correctly taken as a lower limit.);  ${}^{41}\text{Ca}$ : Srinivasan et al. (1996) (This ratio was measured in a CAI with a measured  ${}^{26}\text{Al}/{}^{27}\text{Al}$  ratio that was consistent, within the error bars, with our assumed value. However, it is important to note that if that particular CAI formed late, even by a small amount, the measured  ${}^{41}\text{Ca}$  abundance ratio would be heavily impacted. Again, this ratio is more correctly taken as a lower limit.);  ${}^{53}\text{Mn}$ : Nyquist et al. (1999);  ${}^{60}\text{Fe}$ : Tachibana et al. (2006);  ${}^{107}\text{Pd}$ : Hauri et al. (2000); Carlson & Hauri (2001) (There is a suggestion that the initial abundance ratio may have been as high as  $40 \times 10^{-5}$ .);  ${}^{129}\text{I}$ : Brazzle (1999);  ${}^{146}\text{Sm}$ : Lugmair & Galer (1992);  ${}^{182}\text{Hf}$ : Kleine et al. (2005, 2006). Often the published error bars are  $2\sigma$ , but to be conservative we used the errors as  $1\sigma$ . If the estimated error was less than 10%, we used a conservative 10% error.

<sup>c</sup>From Table 2 Lodders (2003), using the initial solar system abundances, i.e. correction for gravitational settling.

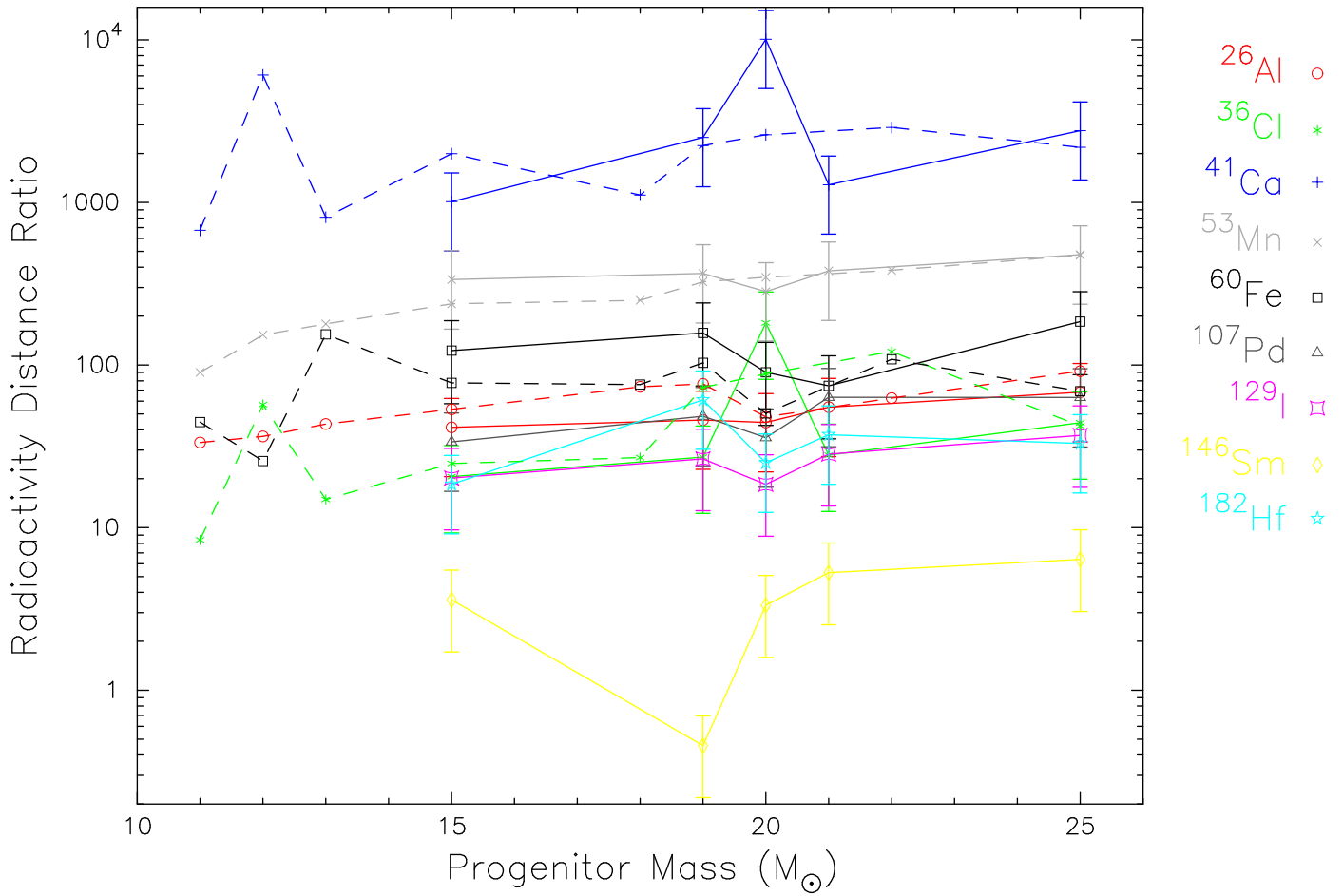


Fig. 1.— The radioactive distance ratio without any decay time. The supernova production models of Woosley & Weaver (1995), dotted lines, and Rauscher et al. (2002), solid lines, are used. The estimated error for each data point is shown only for the Rauscher et al. (2002) models in order to minimize confusion in the Figure.

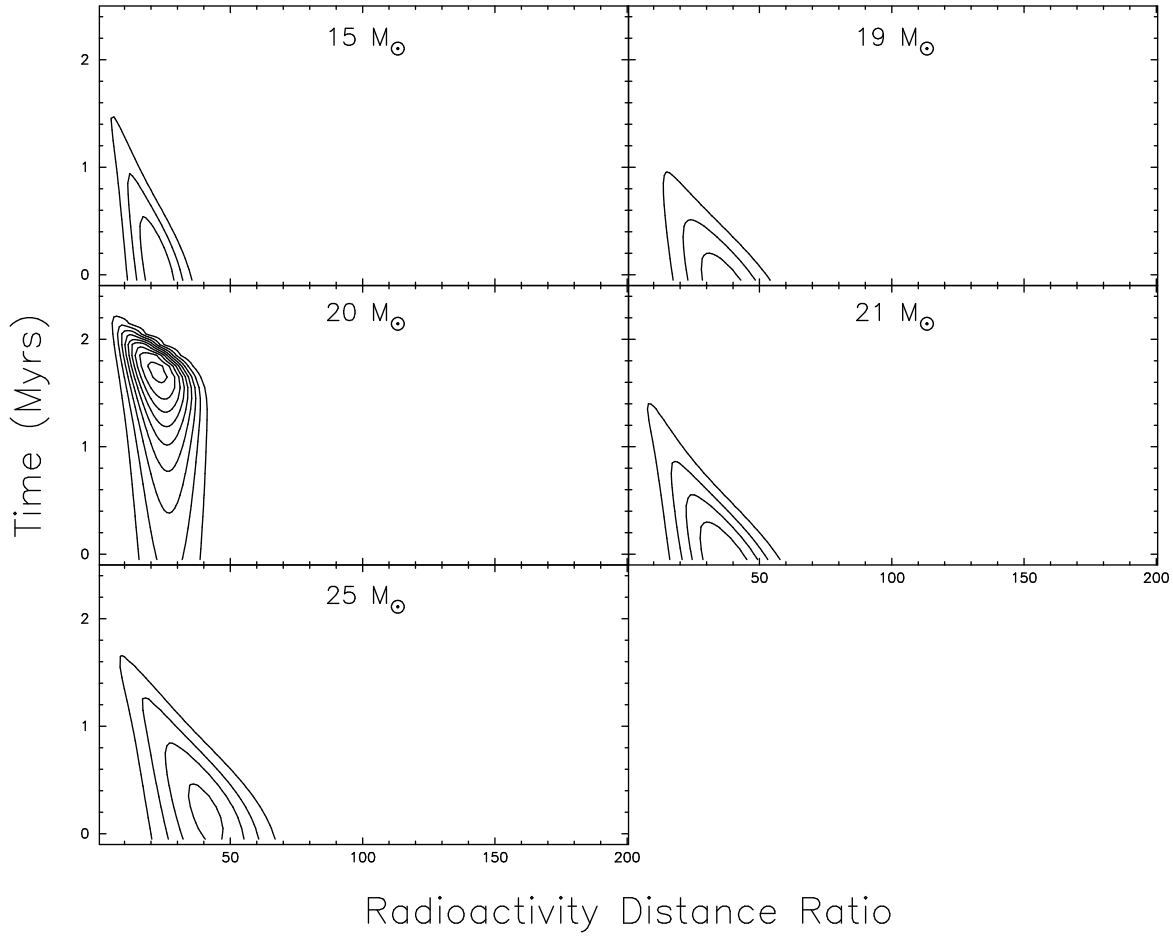


Fig. 2.— The likelihoods of the  $\chi^2$  parameter search for 5 of the models in Rauscher et al. (2002). The mass of the progenitor in the model is listed in each panel. The x-axis is the radioactivity distance ratio: from 1 to 200 in steps of 1. The y-axis is the time delay from ejection to incorporation into CAIs: from 0 to 2.5 Myrs in steps of 0.1. The contours of likelihood are in 10 to 90% in steps of 10%.

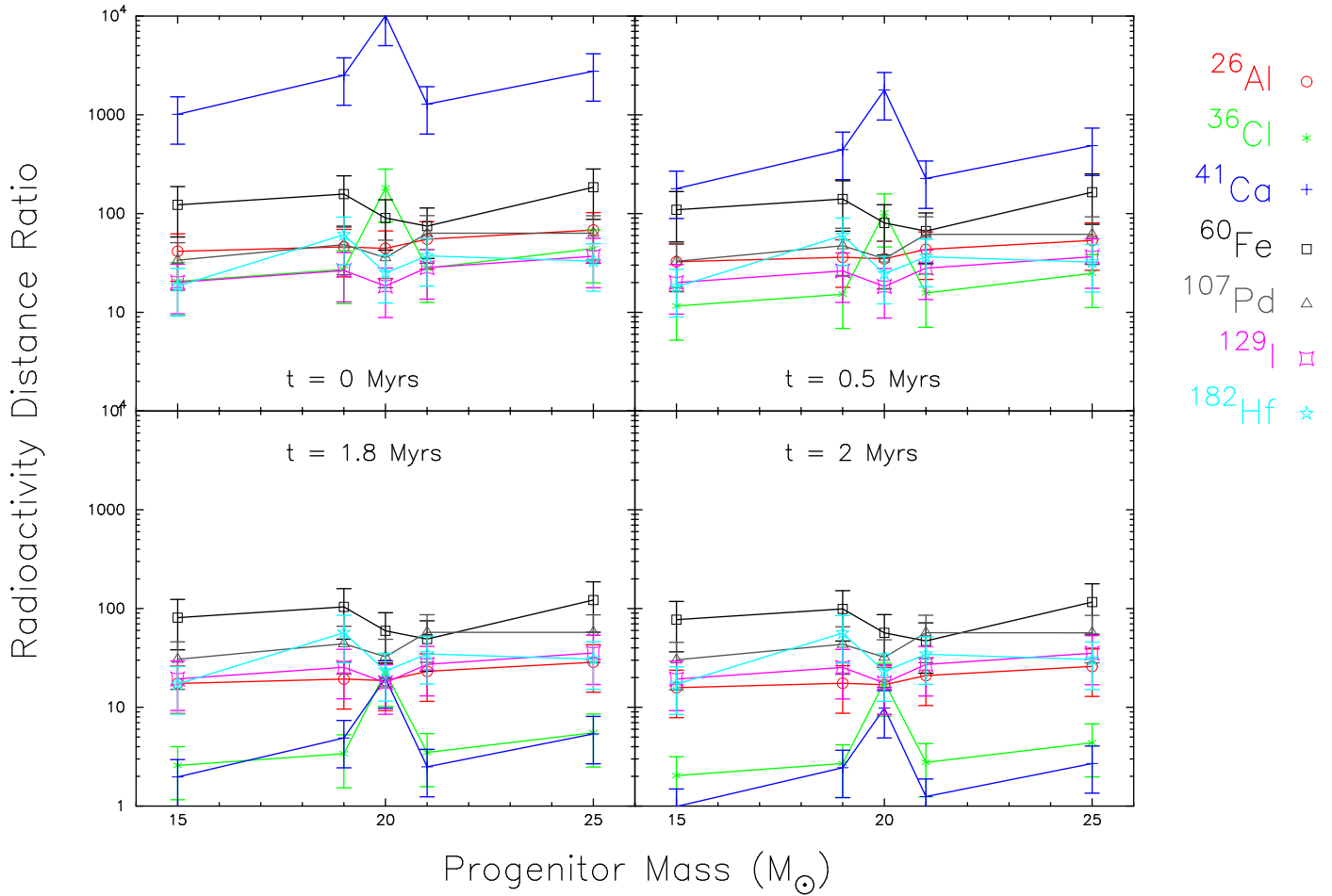


Fig. 3.— The Radioactive Distance ratio with a decay time of 0, 0.1, 1.8, and 2 Myrs for the Rauscher et al. (2002) radionucleosynthesis model. Note that  $^{146}\text{Sm}$  and  $^{53}\text{Mn}$  have been excluded for reasons described in the text.